Materials Letters 118 (2014) 134–136

Contents lists available at ScienceDirect

Materials Letters

journal homepage: www.elsevier.com/locate/matlet

Optical properties of silicon nanocavity-coupled hybrid plasmonic–photonic crystals in the optical region

Zheng-Qi Liu [a], Gui-Qiang Liu [a,*], Xiao-Shan Liu [a], Jin Chen [b], Ying Hu [a], Xiang-Nan Zhang [a], Zheng-Jie Cai [a]

[a] Laboratory of Nanomaterials and Sensors, College of Physics and Communication Electronics, Jiangxi Normal University, Nanchang 330022, China
[b] College of Electronic Science and Engineering, Nanjing University of Posts and Telecommunications, Nanjing 210023, China

ARTICLE INFO

Article history:
Received 23 November 2013
Accepted 19 December 2013
Available online 27 December 2013

Keywords:
Optical materials and properties
Metallic composites
Microstructures

ABSTRACT

Hybrid plasmonic–photonic crystals (HPPCs) have attracted considerable attention due to the cooperative effects of unique plasmonic and photonic features of the plasmonic and photonic crystals. In this work, we fabricate a novel HPPC by intercalating amorphous silicon nanocavities (Si-NCs) between the corrugated metallic plasmonic crystal and the colloidal crystal (CC). Multiple intensified transmission bands are experimentally observed through enhanced optical field coupling of the plasmon modes localized at the metal layer to the eigen modes in the CC by strong electric response of Si-NCs. Significant transmission modifications of such a structure can be efficiently tailored by tuning the geometry of Si-NCs. Calculated transmission spectra also demonstrate these. Our findings might provide potential applications in light harvesting and optoelectronic detections.

1. Introduction

Periodic plasmonic structures have attracted great attention due to their strong light confinement and management via the electronic excitation of large oscillator strength [1]. Currently, the well-known periodic plasmonic structures have been fabricated by coating a metal film on the two-dimensional (2D) colloidal crystals (CCs) [2,3]. In such structures, extraordinary optical transmission (EOT) [4] has been observed and shown various applications [5–7]. EOT has also been widely studied in 2D planar perforated metallic films with different shapes [8–12]. However, in comparison with that of the non-plannar structures [2,3], it has been shown that such in-plane tuning of optical properties via the geometry changes of metallic elements restricts the enhancement of optical transmission. To date, though many investigations are concentrated on the optical modification of the hybrid plasmonic crystals (PCs) by tuning the thickness or geometry shapes of the coated metallic materials [2], far less attention is conducted on the exploration of new unique optical properties via tuning the dielectrics [13].

In this work, we for the first time design and fabricate a novel Si-NC-coupled HPPC in which the Si-NCs are located between the corrugated metal film and the CC. Both theoretical and experimental results show significant transmission modifications by tuning the geometry parameters of Si-NCs. Moreover, EOT can be significantly intensified within a suitable thickness range of Si-NCs due to strong optical field coupling and confinement. Our findings might provide potential applications in sub-wavelength nano-optics, nano-plasmonics, and surface enhanced spectroscopies.

2. Experimental details

A high-quality 2D CC consisting of monodisperse polystyrene (PS) spheres with diameters of 1.02 μm (purchased from Duke Scientific) is self-assembled on a quartz substrate [14–16]. Si-NCs with controllable thickness (t) are then plasma sputtered on top of this CC to form a cap-shape film on CC (denoted as hetero-colloidal crystal, HCC). Finally, a 60 nm gold film is deposited on top of the HCC by vacuum deposition. The thicknesses of Si-NCs and gold film are controlled by the deposition time and confirmed by the deposited thickness on a flat substrate in the same time [2,13]. Numerous simulations are performed using the finite-difference time-domain method [17]. The dielectric constants of PS colloids and Si-NCs are assumed to be $\varepsilon_1 = 2.46$ and $\varepsilon_2 = 12.25$, respectively. The Drude model is used to describe the dielectric constant of the gold to fit the experimental data [18].

3. Results and discussion

Fig. 1(a) shows the optical photo of the CC and the diffractive image obtained by a laser with 633 nm irradiation onto the CC (see the inset), both verifying the high-quality of the CC. A hexagonal-close-packed

* Corresponding author. Tel.: +86 7918120370.
E-mail address: liugq83@163.com (G.-Q. Liu).

0167-577X/$ - see front matter © 2013 Elsevier B.V. All rights reserved.
http://dx.doi.org/10.1016/j.matlet.2013.12.078

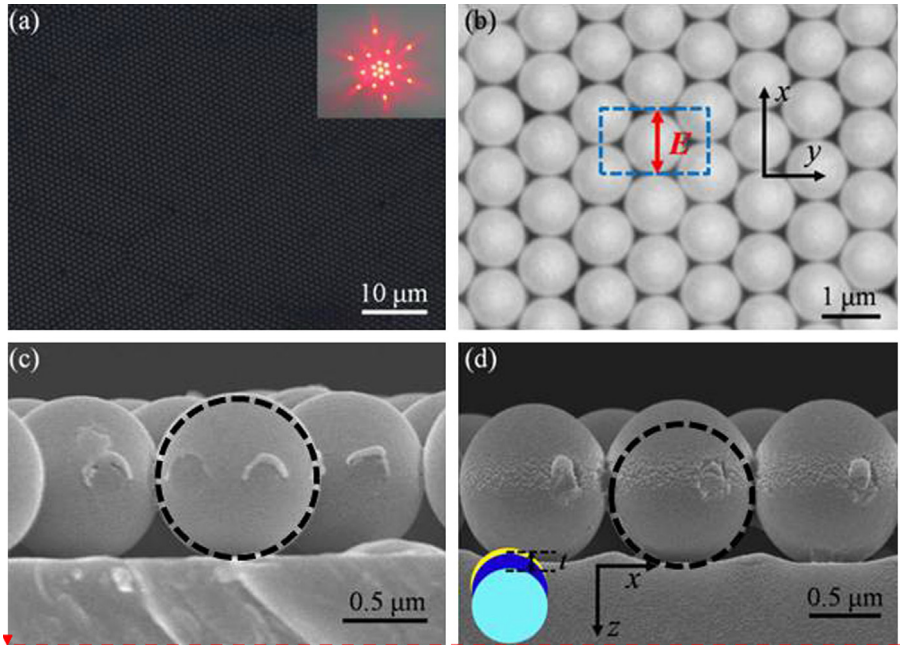

Fig. 1. (a) Optical photo of the large-area 2D CC and its diffractive image. (b) Top-and (c) cross-view SEM images of the PC without the intercalated Si-NCs. Inset: unit cell and electric field polarization along the *x* axis. (d) Cross-view SEM image of the PC with the intercalated Si-NCs.

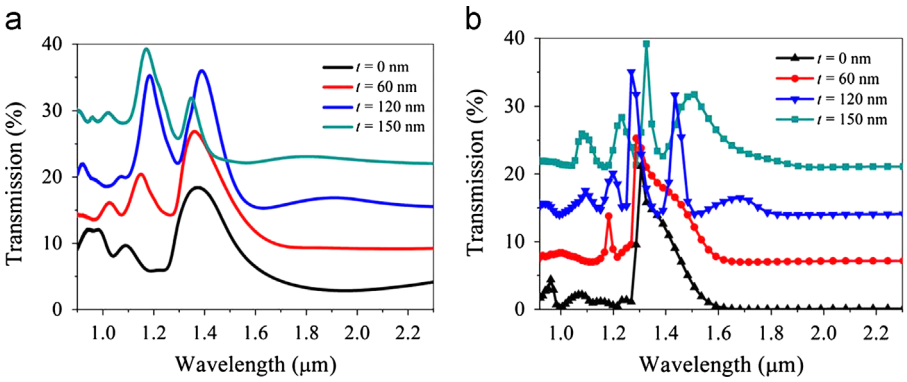

Fig. 2. Measured (a) and calculated (b) transmission spectra of the HPPCs with different *t*. Individual spectra are offset by 7% from one another.

monolayer array of the conventional PC without the intercalated Si-NCs is clearly observed from its SEM images shown in Fig. 1((b) and (c)). The inset in Fig. 1(b) shows the unit cell and the electric field polarization along the *x* axis. Compared with the conventional PC in Fig. 1(c), the HPPC with the intercalated Si-NCs in Fig. 1(d) shows that the deposited Si-NCs are non-uniform in the thickness. The normal thickness (t) along the z axis is defined as the distance between the top of the Si-NC to the top of the PS sphere (see the inset).

Fig. 2(a) shows the measured transmission spectra of the HPPCs including semi-shell Si-NCs with different t. With $t=60$ nm, a strong EOT peak is observed at $\lambda=1360$ nm, almost the same with that of the conventional PC. In addition, an enhanced transmission peak emerges at the shorter wavelength range where there is no obvious transmission peak before. When t is 120 nm, double strong EOT peaks are observed. It should be noted that since there is a buffer dielectric layer intercalated between the gold cover layer and CC, the transmission is weakened due to the reduced coupling between the surface plasmon modes and the photonic engine modes of the CC [2,3]. Therefore, the double strong EOT peaks especially for the shorter wavelength peak observed in Fig. 2(a) suggests other contributions to the enhanced transmission by the high refractive index silicon film. When t is 150 nm, a much weaker EOT peak at $\lambda=1343$ nm and a strongly EOT peak at $\lambda=1172$ nm are observed. The reduced transmission may result from the weakened coupling between the gold semi-shells and CC due to the large spatial separation by the Si-NCs. Fig. 2(b) shows the calculated transmission spectra for the HPPCs with approximate geometry thickness t obtained from the experimental measurements. It is seen that the calculation results reproduce the measured optical features well. The calculation results predict strong EOT modifications by tuning the thickness of the intercalated Si-NCs. Particularly, double strong EOT bands could be achieved in a suitable thickness range, providing potential applications in surface enhanced Raman scattering [19,20] and light harvesting [21,22].

Based on the calculated model, we further study the physical mechanisms of the strong modification of EOT in the Si-NC-coupled HPPCs by analyzing the corresponding electric field intensity $|E|^2$ distributions of the main transmission peaks. The simulation unit cell and the polarization direction of incident light are shown in Fig. 3(a). The cross-sectional electric field distributions of the EOT peaks located at $\lambda=1306$ nm and $\lambda=1067$ nm of the structure without the Si-NCs are respectively presented in Fig. 3(b) and (c), which are known to be the results of the

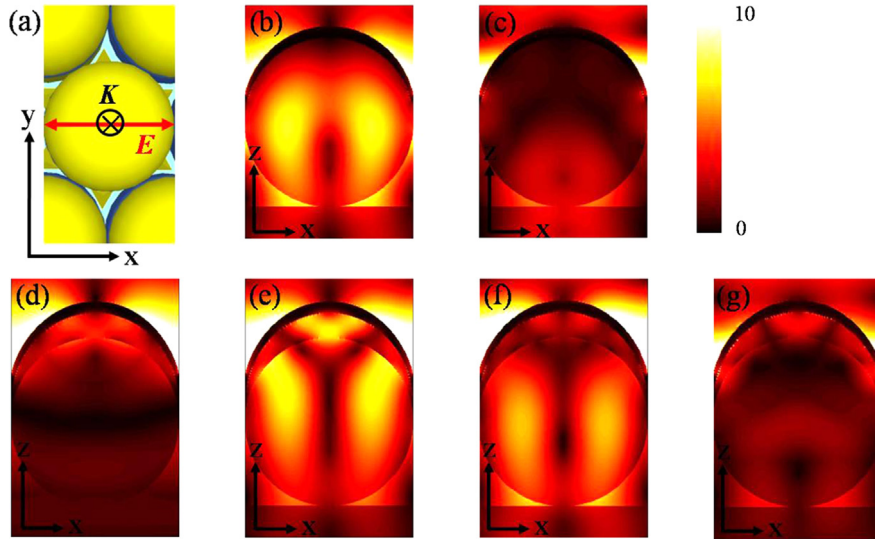

Fig. 3. (a) Simulation unit cell with the linear polarization illumination along the z axis and the electric polarization along the x axis. Calculated Electric field intensity $|E|^2$ distributions of the structure with $t=0$ nm at $\lambda=1306$ nm (b) and $\lambda=1067$ nm (c), and with $t=150$ nm at $\lambda=1483$ nm (d), 1326 nm (e), 1250 nm (f), 1090 nm (g), respectively.

excitation of sphere-like localized plasmon resonance modes and the photonic eigen modes of the CC [2,3].

Fig. 3((d)–(g)) present the electric field distributions of the proposed structure with 150 nm Si-NCs at $\lambda=1483$ nm, 1326 nm, 1250 nm, and 1090 nm (as shown in Fig. 2), respectively. At $\lambda=1483$ nm, besides the strong electric field intensity confined at the outside of the gold layer, obvious electric field intensity distributions are observed in the intercalated Si-NCs (Fig. 3(d)), which suggest that the enhanced EOT peak mainly results from the excitation of photonic mode supported by the Si-NCs. Strong electric field in the Si-NCs and strong coupling between the Si-NCs and CC suggest the intercalated high refractive index dielectrics could efficiently couple to the optical field and significantly modify the light-matter interaction [23]. Strong electric field distributions in the Si-NCs also show that the intercalated Si-NCs could even enhance the coupling between the top gold layer and the bottom CC due to its high efficient light coupling and confinement capability [23,24]. At $\lambda=1250$ nm, the whole electric field distribution patterns (Fig. 3(f)) are very similar to those of the EOT peak at $\lambda=1326$ nm (Fig. 3(e)) due to the degenerate states of the EOT mode. At $\lambda=1090$ nm (Fig. 3(g)), strong electric field intensity confined in the Si-NCs suggests the relevance of photonic modes in the Si-NCs to this EOT peak.

4. Conclusions

We have proposed and fabricated a novel HPPC to achieve significant modification of EOT phenomena. By intercalating the Si-NCs between the top metal semi-shells and the bottom CC, multiple enhanced EOT bands are achieved. The EOT peaks could be efficiently modified by tuning the thickness of the dielectric film. Our findings might be helpful to understand the mechanisms of EOT in these metallic structures, and also to further exploit large-area and low-cost structures in sub-wavelength optics, plasmonics, and surface enhanced spectroscopies.

Acknowledgements

Work was funded by the National Natural Science Foundation of China (Nos. 11004088, 11264017, 11304059), Natural Science Foundation of Jiangxi Province (No. 20122BAB202006), Scientific and Technological Supporting Projects of Jiangxi Province (No. 20112BBE50033), and Scientific and Technological Projects of Jiangxi Provincial Education Department (No. GJJ13234).

References

[1] García-Vidal FJ, Martín-Moreno L, Ebbesen TW, Kuipers L. Rev Mod Phys 2010;82:729–87.
[2] Romanov SG, Korovin AV, Regensburger A, Peschel U. Adv Mater 2011;23:2515–33.
[3] Farcau C, Astilean S. J Opt A: Pure Appl Opt 2007;9:S345–9.
[4] Ebbesen TW, Lezec HJ, Ghaemi HF, Thio T, Wolff PA. Nature 1998;391:667–9.
[5] Zhu X, Xie F, Shi L, Liu X, Mortensen NA, Xiao S, et al. Opt Lett 2012;37:2037–9.
[6] Zhao Y, Zhang XJ, Ye J, Chen LM, Lau SP, Zhang WJ, et al. ACS Nano 2011;5:3027–33.
[7] He L, Huang J, Xu T, Chen L, Zhang K, Han S, et al. J Mater Chem 2012;22:1370–4.
[8] Wang QJ, Liu JQ, Huang CP, Zhang C, Zhu YY. Appl Phys Lett 2005;87:091105.
[9] Liu JQ, He MD, Zhai X, Wang LL, Wen S, Chen L, et al. Opt Express 2009;17:1859–64.
[10] Klein Koerkamp KJ, Enoch S, Segerink FB, van Hulst NF, Kuipers L. Phys Rev Lett 2004;92:183901.
[11] Wang C, Gu J, Han J, Xing Q, Tian Z, Liu F, et al. Appl Phys Lett 2010;96:251102.
[12] Orbons SM, Roberts A. Opt Express 2006;14:12623–8.
[13] Yu X, Shi L, Han D, Zi J, Braun PV. Adv Funct Mater 2010;20:1910–6.
[14] Wang A, Chen SL, Dong P. Mater Lett 2009;63:1586–9.
[15] Liu ZQ, Feng TH, Dai QF, Wu LJ, Lan S. Chin Phys B 2009;18:2383–8.
[16] Liu GQ, Liu ZQ, Huang K, Chen YH, Li L, Tang FL, et al. Mater Lett 2013;93:42–4.
[17] Liu ZQ, Liu GQ, Zhou HQ, Liu XS, Huang K, Chen YH, et al. Nanotechnology 2013;24:155203.
[18] Johnson PB, Christy RW. Phys Rev B: Condens Matter 1972;6:4370–9.
[19] Chu Y, Banaee MG, Crozier KB. ACS Nano 2010;4:2804–10.
[20] Chanda D, Shigeta K, Truong T, Lui E, Mihi A, Schulmerich M, et al. Nat Commun 2011;2:479.
[21] Yao Y, Yao J, Narasimhan V K, Ruan Z, Xie C, Fan S, et al. Nat Commun 2012;3:664.
[22] Shi L, Harris J T, Fenollosa R, Rodriguez I, Lu X, Korgel BA, et al. Nat Commun 2013;4:1904.
[23] Yang X, Ishikawa A, Yin X, Zhang X. ACS Nano 2011;5:2831–8.
[24] Barth M, Schietinger S, Fischer S, Becker J, Nüsse N, Aichele T, et al. Nano Lett 2010;10:891–5.